Differential effects of N-glycans on surface expression suggest structural differences between acid-sensing ion channel (ASIC) 1a and ASIC1b

Ivan Kadurin, Andjelko Golubovic, Lilia Leisle, Hermann Schindelin, Stefan Gründer

Differential effects of *N*-glycans on surface expression suggest structural differences between acid-sensing ion channel (ASIC) 1a and ASIC1b

Ivan KADURIN*, Andjelko GOLUBOVIC*, Lilia LEISLE*[1], Hermann SCHINDELIN†, and Stefan GRÜNDER*[2]

*Institute of Physiology II, University of Würzburg, Röntgenring 9, D-97070 Würzburg, Germany, †Rudolf Virchow Center for Experimental Biomedicine and Institute of Structural Biology, University of Würzburg, Versbacher Strasse 9, 97078 Würzburg, Germany

[1] Present address: Labor für Medizinische Genomforschung, Leibniz-Institut für Molekulare Pharmakologie and Max-Delbrück-Centrum für Molekulare Medizin, Robert-Roessle-Strasse 10, D-13125 Berlin, Germany

[2] Address correspondence to: Stefan Gründer, Institute of Physiology, RWTH Aachen University, Pauwelsstr. 30, D-52074 Aachen, Germany, Tel.: +49 241-80-88800; Fax: +49 241-80-82434; E-mail: sgruender@ukaachen.de

Abbreviations used: ASIC, acid-sensing ion channel; Endo H, endoglycosidase H; HA, hemagglutinin; MES, 2-(*N*-morpholino)ethanesulfonic acid; PNGase F, *N*-glycosidase F;

Short title: Glycosylation of ASIC1

Acid-sensing ion channels (ASICs) are H^+-gated Na^+ channels, with a widespread expression pattern in the central and the peripheral nervous system. ASICs have a simple topology with two transmembrane domains, cytoplasmic termini, and a large ectodomain between the transmembrane domains; this topology has been confirmed by the crystal structure of chicken ASIC. ASIC1a and ASIC1b are two variants encoded by the *asic1* gene. The variable part of the protein includes the cytoplasmic N-terminus, the first transmembrane domain and approximately the first third of the ectodomain. Both variants contain two consensus sequences for *N*-linked glycosylation in the common, distal part of the ectodomain. In contrast to ASIC1a, ASIC1b contains two additional consensus sequences in the variable, proximal part of the ectodomain. Here we show that all extracellular Asn residues within putative consensus sequences for *N*-glycosylation carry glycans. The two common, distal glycans increase surface expression of the channels but are no absolute requirement for channel activity. In sharp contrast, the presence of at least one of the two proximal glycans, which are specific to ASIC1b, is an absolute requirement for surface expression of ASIC1b. This result suggests substantial differences in the structure of the proximal ectodomain between the two ASIC1 variants.

Key words: ASIC, acid-sensing ion channel, *N*-glycans, trafficking, structure

INTRODUCTION

Acid-sensing ion channels are H^+-gated Na^+ channels [1]. They are abundantly expressed in the central and peripheral nervous system and have a role in synaptic transmission and sensory transduction [2, 3]. In mammals, six ASICs are generated from four *asic* genes. They all share a simple topology with two transmembrane domains (M1 and M2), a large ectodomain (> 350 amino acids) and relatively short (40 - 90 amino acids) cytoplasmic termini [4]. This topology has been confirmed by the recently determined crystal structure of a chicken ASIC1 deletion mutant [5]. Moreover, the ASIC1 crystal revealed that three subunits assemble into the functional channel. The extracellular region is composed of five subdomains, which are connected to the membrane-spanning region via an apparently flexible wrist [5]; as previously predicted [6], this region is stabilized by cysteine-bridges formed by 14 highly conserved cysteines.

ASIC1a and ASIC1b derive from the *asic1* gene, probably by using alternative promoters; the N-terminal third of the proteins is different, including the intracellular N-terminus, the first transmembrane domain and the proximal part of the ectodomain [7, 8]. ASIC1a is broadly expressed in the central and peripheral nervous system [9], whereas ASIC1b is specifically expressed in the peripheral nervous system [7]. There are also functional differences between the two variants. ASIC1a is the only ASIC that is permeable for Ca^{2+} [8-10]; the lack of Ca^{2+} permeability of ASIC1b can be attributed to differences in a pre-M1 region [8]. Moreover, ASIC1a has a higher apparent H^+ affinity than ASIC1b, which is due to differences in a short stretch of amino acids after M1 [11]. Finally, ASIC1b has a much longer cytoplasmic N-terminus than ASIC1a (88 compared to 43 amino acids) [8]; the first 15 amino acids of the ASIC1b N-terminus are conserved in ASIC4 [12, 13] and may have an unknown functional role [14].

Most membrane proteins are glycoproteins and *N*-glycans can serve many functions. Among them, they can aid the proper folding of the protein, stabilize the structure of the protein, and promote its intracellular trafficking [15, 16]. Some glycoproteins strictly depend on *N*-glycans for their function [17-19] whereas for other glycoproteins *N*-glycans are completely dispensable.

All ASICs have at least one consensus site for *N*-glycosylation (Asn-X-Ser/Thr, where X is any amino acid except Pro). Glycosylation has been investigated for ASIC2a [4]. Both consensus sites for glycosylation in the ectodomain of ASIC2a (Fig. 1A) are used. Removal of the first *N*-glycan (at N365) has no effect on current amplitude or apparent H^+ affinity, whereas removal of the second glycan (at N392) reduces current amplitude 2-fold. Removal of both glycans together reduces current amplitude 3-fold and apparent H^+ affinity by 0.6 pH units [4]. These results show that although glycans are necessary for the full activity and H^+ affinity of ASIC2a, they are no absolute requirement for channel activity. Apparently, ASIC2a devoid of glycans can assemble into oligomeric channels, traffic to the cells surface and form functional H^+-gated channels.

The two glycosylation sites of ASIC2a are conserved in ASIC1a and ASIC1b (Fig. 1A). ASIC1b, but not ASIC1a, has two additional glycosylation consensus sites in the alternative, proximal part of the ectodomain. In the present study we investigated the glycosylation pattern of ASIC1a and ASIC1b. We found that all Asn residues within potential extracellular glycosylation sites of ASIC1a and 1b carry glycans. The two distal *N*-glycans, which are shared with ASIC2a, are not absolutely required for channel activity. Surprisingly, however, one glycan at either of the two proximal sites of ASIC1b is mandatory for surface expression of ASIC1b. We propose that the proximal glycans are essential for the proper folding of ASIC1b, suggesting substantial structural differences in the proximal part of the ectodomain of ASIC1a and ASIC1b.

MATERIALS AND METHODS

cDNAs and Site-directed Mutagenesis

cDNAs for rat ASIC1a and ASIC1b have been described previously [8]. The point mutations were constructed by recombinant PCR using Pwo DNA polymerase (Roche Applied Science). In some experiments, ASIC1a was tagged with the hemagglutinin (HA) epitope (YPYDVPDYA); ASIC1b was always tagged with the HA and the vesicular stomatitis virus glycoprotein (VSV-G) epitope (YTDIEMNRLGK). The HA-epitope was inserted into the extracellular loop of the proteins – for ASIC1a between F147 and K148 and for ASIC1b between F180 and S181. Thus, according to the crystal structure of chicken ASIC [5], the epitopes localize to a loop between α helix 1 and α helix2 of the finger subdomain, where they should be well accessible (Fig 1B). Introduction of the HA-epitope required injection of larger amounts of cRNA for current amplitudes comparable to the wild-type (ASIC1a ~10-fold and ASIC1b ~2-fold larger amounts). The VSV-G epitope was added in frame to the C terminus of ASIC1b; introduction of the VSV-G epitope did not alter functional expression of the channel. All PCR-derived fragments were entirely sequenced (MWG-Biotech).

Maintenance of oocytes

Animal care and experiments followed approved institutional guidelines at the University of Würzburg. Ovaries were surgically removed under anaesthesia from adult *Xenopus laevis* females and oocytes were isolated. Using mMessage mMachine (Ambion, Austin, TX), capped cRNA was synthesized by SP6 RNA polymerase from cDNAs, which had been linearized by Nae I. cRNA was injected into oocytes of *Xenopus laevis;* after injection, oocytes were kept in OR-2 medium (concentrations in mM: 82.5 NaCl, 2.5 KCl, 1.0 Na_2HPO_4, 5.0 HEPES, 1.0 $MgCl_2$, 1.0 $CaCl_2$, and 0.5 g/liter polyvinylpyrrolidone) at 19°C.

Immunoblot analysis

0.1-10 ng of cRNA coding for the tagged proteins was injected into oocytes. Microsomal membranes were prepared 2 days after injection as previously described [20]. Some samples were treated with Endo H (Roche) in a sodium citrate buffer (150 mM, pH 5.5) or with PNGase F (Roche) in a sodium phosphate buffer (80 mM, pH 8.0) in the presence of 1% Triton X100. Proteins from microsomal membranes of two oocytes were separated on a 8-14 % gradient polyacrylamide-SDS gel and transferred to a polyvinylidene fluoride membrane (PolyScreen; PerkinElmer Life Sciences). Either peroxidase-coupled anti-HA antibody (1:1000; Roche Applied Science) or anti-VSV-G antibody (0,5 µg/ml; Roche Applied Science) in combination with peroxidase-coupled anti-mouse antibody (1:5000; Santa Cruz Biotechnology, Inc., Santa Cruz, CA) was used for detection. Bound antibodies were revealed by chemiluminescence (ECL kit, GE Healthcare).

Electrophysiology

1-10 ng of ASIC1b cRNA and 0.01 ng of ASIC1a cRNA was injected into individual *Xenopus* oocytes. 24-48 hours after injection, whole-cell currents were measured using two-electrode voltage-clamp as previously described [21]. During recording, oocytes were bathed in solutions containing (in mM): 140 NaCl, 1.8 $CaCl_2$, 1.0 $MgCl_2$, 10 HEPES, pH as indicated in figures. For solutions with a pH lower than 6.8, HEPES was replaced by MES. Membrane voltage was held at –70 mV. Data were filtered at 50 Hz and acquired at 0.1-1 kHz. All measurements were performed at room temperature (20-25 °C).

Data were analyzed with the software IgorPro (Wave metrics). pH response curves were fit with a Hill function:

$$I = a + (I_{max} - a)/\left(1 + (EC_{50}/[H])^n\right),$$

where I_{max} is the maximal current, a is the residual current, [H] is the H^+-concentration, EC_{50} is the half-maximal response occurs, and n is the Hill coefficient. Before fitting, current amplitudes were normalized to the amplitude at the lowest pH used; I_{max} was fixed to 1. The pH of half-maximal activation, pH_{50}, was calculated as $-\log(EC_{50})$. Time constants of desensitization were determined by fitting the decay phase of current traces to a mono-exponential function. Results are reported as means ± SEM. Statistical analysis was done with the unpaired *t*-test.

Quantification of surface expression

10 ng of cRNA coding for ASIC1b constructs were injected into *Xenopus laevis* oocytes. After 2 days of protein expression at 19°C, the surface expression of the HA-tagged ASIC1b constructs was determined as previously described [22]. Rat anti-HA antibody (clone 3F10; 1:200; Roche) and HRP-conjugated anti-rat antibody (1:400; Jackson ImmunoResearch Laboratories) were used to label the surface expressed HA-tagged ASIC1b constructs. Single oocyte chemiluminescence was detected with an Orion II Microplate Luminometer (Berthold detection systems; Pforzheim, Germany) in relative light units (RLUs) per sec. RLUs of HA-tagged channels were at least 100-fold higher than RLUs of untagged channels. Results from three different batches of oocytes (for each: n = 5-14) are reported as mean ± S.E.M. Statistical analysis was performed with the unpaired *t*-test.

RESULTS

ASIC1a is a glycoprotein, which carries two glycans

Rat ASIC1a has a predicted molecular mass of ~60 kD. The inserted HA epitope should increase the molecular weight to ~61 kD. But immunoblot analysis of membrane protein extracts from *Xenopus* oocytes injected with HA-tagged ASIC1a revealed an apparent molecular weight of more than 70 kD for this protein (Fig. 2B, lanes 1 and 4). Treatment of protein extracts with endoglycosidase H (Endo H) or *N*-glycosidase F (PNGase F) reduced the apparent molecular mass of ASIC1a by a few kD (Fig. 2B, lanes 2 and 3), demonstrating that ASIC1a is a glycoprotein. There are two types of *N*-glycans: high mannose-type, synthesized in the ER, and complex- or mature-type glycans, which result from further processing of high-mannose glycans in the Golgi apparatus. Endo H selectively removes high mannose-type sugars, while PNGase F removes both types of *N*-glycans. We found no evidence for an Endo H resistant form of ASIC1a, suggesting that high mannose-type ASIC1a traffics to the oocyte plasma membrane without further modification of the sugars in the Golgi. Alternatively, the complex-type form may be too rare to be detected. Closer inspection of the ASIC1a immunoreactivity shows that ASIC1a ran as a double band (Fig.2B, lanes 1 and 4); after glycosidase treatment, however, only a single band could be observed (Fig.2B, lanes 2 and 3), suggesting that the ASIC1a population was heterogeneous with respect to *N*-glycans.

ASIC1a has two consensus sequences for *N*-glycosylation (NXS/T): one at N366 and one at N393, both in the distal part of the ectodomain (Fig. 2A). Individual substitution of N366 and N393 slightly reduced the apparent molecular mass of ASIC1a and combined substitution of both residues further reduced the molecular mass (Fig. 2C, lanes 2, 3 and 4), showing that both potential glycosylation sites are used. Closer inspection reveals that the N366A (Fig. 2C, lane 2) mutant ran as a single band whereas the N393S mutant ran as a

doublet (Fig. 2C, lane 3), like wild-type ASIC1a . Overall these results suggest that one part of the ASIC1a population carries sugars at both glycosylation sites (N366 and N393) whereas the other part of the population carries sugars only at N393. Such inefficient glycosylation of N366 could, for example, be due to rapid folding and sequestering of the consensus site [23]. In summary, N393 seems to be the prime glycosylation site of ASIC1a.

N-glycosylation is dispensable for ASIC1a function

We next studied the implications of *N*-glycans on the function of ASIC1a by measuring whole cell currents of oocytes expressing ASIC1a with substitutions at the glycosylation consensus sites. Expression of ASIC1a mutants N366A and N393S, as well as of the double mutant N366A/N393S gave rise to pH gated currents (Fig. 3A). Desensitization of mutants N366A and N393S had a tendency to be faster than desensitization of ASIC1a (desensitization time constant τ = 1.7 ± 0.4 sec and 1.7 ± 0.3 sec, respectively, compared to 2.1 ± 0.4 sec; $p > 0.1$; $n = 12$); desensitization of double mutant N366A/N393S was significantly faster than desensitization of ASIC1a (τ = 1.1 ± 0.1 sec; $p = 0.01$; $n = 12$). Moreover, current amplitudes were reduced compared to the wild type channels (Fig. 3B): the N366A substitution reduced the amplitude about 2-fold, the N393S substitution about 3-fold, and the double-substitution also about 2-fold. All three mutant channels had a slightly but significantly ($p \leq 0.05$) lower apparent H^+-affinity than wild-type channels (Fig. 3C): the pH_{50} was shifted from pH 6.43 ± 0.02 for ASIC1a wild-type to 6.36 ± 0.02 for ASIC1a-N366A, to 6.32 ± 0.03 for ASIC1a-N393S, and to 6.33 ± 0.02 for the double mutant N366A/N393S (n = 12). The reduction in apparent affinity was especially evident at low H^+ concentrations (Fig. 3C).

In summary, although *N*-glycans slowed desensitization, increased ASIC1a current amplitude and apparent H^+ affinity, they were largely dispensable for ASIC1a function, similar to the *N*-glycans of ASIC2a [4].

ASIC1b is a glycoprotein with four N-glycans

Rat ASIC1b has a predicted molecular mass of ~62 kD [8]. Insertion of the hemagglutinin (HA) epitope in the extracellular loop should increase the molecular mass to ~63 kD. In addition, ASIC1b was tagged at its C-terminus with the vesicular stomatitis virus-glycoprotein (VSV-G) epitope, further increasing the predicted molecular mass to ~65 kD. Immunoblot analysis revealed an apparent molecular mass of ~70 kD for HA- and VSV-tagged ASIC1b (Fig. 4B, lanes 1 and 4). Treatment of protein extracts with Endo H and PNGase F reduced the apparent molecular mass of ASIC1b by several kD (Fig. 4B, lanes 2 and 3), demonstrating that also ASIC1b is a glycoprotein. As for ASIC1a, we found no evidence for an Endo H resistant form of ASIC1b. In contrast to ASIC1a, however, the ASIC1b population seemed to be homogenous with respect to *N*-glycans (Fig. 4).

ASIC1b has four consensus sequences for *N*-glycosylation: two of them are in the distal part of the extracellular loop (N399 and N426; Fig. 4A) and are identical to those of ASIC1a. The two others are in the alternatively spliced, proximal part of the protein - one at N192 and one at N216. Individual substitution of the two proximal residues N192 and N216 slightly reduced the apparent molecular mass of ASIC1b and combined substitution of both residues further reduced the molecular mass (Fig. 4C, lanes 2, 3 and 4), suggesting that both sites carry glycans. Individual substitution of residue N399 only slightly reduced the apparent molecular mass of ASIC1b whereas substitution of residue N426 more strongly reduced the apparent molecular mass (Fig.4C, lanes 6 and 7). Combined substitution of both residues did not visibly further reduce the molecular mass compared to substitution of N426 alone (Fig. 4C, lanes 7 and 8). These results suggest that both residues carried a glycan; this glycan seems to be small for N399, however. Since glycans are added in the ER as a preformed 14-

residue oligosaccharide, this interpretation suggests that the glycan at N399 had been further trimmed in the Golgi complex. Combined substitution of all four glycosylation consensus sequences together further reduced the molecular mass of ASIC1b (Fig. 4C, lane 9). In addition, also the total amount of protein was reduced. This reduction of the protein amount suggests reduced protein stability and was consistently observed only for the N1 - N4 construct.

N-glycosylation at one of the proximal sites is indispensable for ASIC1b function

We next studied the implications of *N*-glycans on the function of ASIC1b. We started with the distal glycans at N399 and N426. Substitution of N399 by Ala did not significantly reduce the current amplitude (Fig. 5B). This finding is consistent with its minor posttranslational modification. In contrast, substitution of N426 reduced the current amplitude about 5-fold ($p < 0.01$), similar to its effect on ASIC1a. Combined substitution of the two residues similarly reduced the current amplitude 5-fold ($p < 0.01$). Apparent H^+-affinity was slightly reduced for N399A and the double mutant N399A/N426S (Fig. 5C): the pH_{50} was shifted from pH 5.78 ± 0.01 to 5.72 ± 0.01 ($p < 0.01$) and to 5.69 ± 0.02 ($p < 0.01$), respectively ($n = 12$); there was no significant shift for the single mutant N426S (pH_{50}: 5.76 ± 0.01; $n = 13$; $p = 0.3$). These results show that both distal sites are necessary for the proper working of ASIC1b; a glycan at N399 slightly increased apparent H^+-affinity whereas a glycan at N426 increased current amplitude. Similar to the glycans of ASIC1a and ASIC2a, however, the two distal glycans of ASIC1b were not absolutely required for channel function.

The two proximal sites (N192 and N216) are not present in ASIC1a. Therefore, we expected no dramatic functional effect of substitutions at these two sites. Individual substitution of N192 and N216 reduced the current amplitude 4- to 8-fold ($p < 0.01$), however, similar to the N426 substitution (Fig. 5B). The apparent proton affinity was also reduced: the pH_{50} was shifted from pH 5.63 ± 0.01 ($n = 6$) for ASIC1b wild-type to 5.57 ± 0.03 for N192A ($n = 6$; $p < 0.01$) and to 5.46 ± 0.02 for N216S ($n = 6$; $p < 0.01$; Fig. 5C). Combined substitution of the two residues almost completely silenced the channels (1% of the wild-type amplitude; $p < 0.01$; Fig. 5B), making it impossible to determine an apparent affinity for H^+. This result shows that a glycan at least at one of the two proximal sites is indispensable for ASIC1b activity.

Desensitization was faster for ASIC1b ($\tau = 0.5 \pm 0.02$ sec, $n = 18$; Fig. 5A) than for ASIC1a. Due to the small desensitization time constants it was not possible to determine with precision the effect of *N*-glycans on desensitization kinetics. The two proximal glycans had no significant effect on desensitization, whereas the N399A substitution as well as the N399S/N426A double substitution significantly speeded desensitization ($\tau = 0.4 \pm 0.01$ sec and $\tau = 0.4 \pm 0.02$ sec, respectively; $p < 0.05$; $n = 18$; Fig. 5A), consistent with the faster desensitization of the glycan mutants of ASIC1a (Fig. 3A).

N-glycosylation at one of the proximal sites is indispensable for ASIC1b surface expression

Since substitution of some of the ASIC1b glycosylation sites dramatically reduced the current amplitude, we asked whether these substitutions compromised trafficking of the channels to the plasma membrane. ASIC1b wild-type and mutant channels used in this study carried an HA epitope within the extracellular loop; we used a monoclonal anti-HA antibody and a luminescence assay to compare the surface expression of these channels. As expected from the unchanged current amplitude, surface expression of ASIC1b-N399A was not significantly reduced compared to the wild-type protein (Fig. 6). Surface expression of ASIC1b-N426, however, was reduced ~5-fold (Fig. 6). Additional introduction of the N399 substitution

(ASIC1b N399A/N426S) did not further reduce surface expression. Removing individually the proximal *N*-glycans at N192 and N216 caused a strong decrease in surface expression by a factor of ~5, similar to removal of the distal *N*-glycan at N426. Simultaneous removal of the two proximal *N*-glycans abolished surface expression of the protein. Thus, the reduction in surface expression (Fig. 6) almost perfectly matched the reduction in current amplitude (Fig. 5B), suggesting that the reduced current amplitudes are mainly due to a reduced number of functional ion channels at the plasma membrane rather than to a reduced activity of single ion channels.

Together our results show that ASIC1b carries *N*-glycans at four sites: N192, N216, N399, and N426. The *N*-glycans on N192, N216 and N426 strongly promoted the surface expression of ASIC1b; one glycan either at position N192 or at position N216 was indispensable for the surface expression of ASIC1b.

DISCUSSION

Our study shows that both ASIC1a and ASIC1b are glycoproteins. This was an expected finding. Moreover, the glycosylation pattern of ASIC1a was very similar to the published glycosylation pattern of ASIC2a [4]: both proteins have two conserved consensus sequences for *N*-glycosylation in the distal part of the ectodomain. Both sites carry glycans, which are dispensable for channel activity, however. Even in the absence of any glycan, ASIC1a and ASIC2a are able to assemble into functional oligomeric channels that traffic to the plasma membrane and are gated by H^+. Reduced current amplitude and slightly altered apparent H^+ affinity suggest, however, that the *N*-glycans assist in channel assembly and/or trafficking as well as channel function. The two distal sites are conserved in ASIC1b and have a similar role also for this channel.

The two distal glycosylation sites are also conserved in chicken ASIC1, for which the crystal structure is available [5]. The chicken ASIC1 crystal reveals the position of these two glycans within the three-dimensional structure of an ASIC (Fig. 1B). The first site (corresponding to N366 of rat ASIC1a) is at the beginning of β-sheet 10 within the palm domain whereas the second site (corresponding to N393) is at the end of α-helix 6 of the knuckle domain [5]. Both glycans, though close in the primary sequence, are thus on opposite parts of the ectodomain pointing away from the protein core (Fig. 1B). Hence both glycans seem easily accessible, rendering unlikely the possibility that modifying enzymes of the Golgi complex cannot access these glycans to trim them to complex-type glycans. The position of the two distal glycans at points where the secondary structure of the protein changes is in agreement with a general trend for the frequent occurrence of glycans at such points [24]; glycans may actually favor the reorientation of the peptide chain [24]. The first of these two distal sites is highly conserved in ASICs from rat and fish [21], the one exception is ASIC3, which has the second distal site, however (Fig. 1). Thus, it seems that each ASIC has at least one of the two distal glycosylation sites, suggesting some functional role for the distal glycans.

In this context, it is important to remember that subtle functional impacts of glycans may have been missed in the *Xenopus* oocyte expression system. In a living animal, proteins likely are exposed to other conditions than in *Xenopus* oocytes. Glycans may, therefore, stabilize the protein structure in a living animal although no functional requirement is observed in oocytes. For example, the temperature of 19°C at which we kept the oocytes is well below the body temperature of mammals. Glycans were, however, also dispensable for ASIC2a activity in HEK293 cells [4] cultured at 37°C, arguing against strong temperature-dependent effect of the distal glycans.

The surprise came when analyzing the two proximal sites that are specific for ASIC1b. Eliminating both proximal sites together completely abolished ASIC1b activity; this loss of channel function could be clearly attributed to a loss of surface expression (Fig. 6). There are different possibilities how glycans could promote surface expression: they could assist in folding of the protein, stabilize the protein structure, or promote trafficking to the cell surface. We consider the last possibility as less likely since the related ASIC1a apparently does not need glycans for surface targeting. The first two possibilities (folding of the protein, stabilization of its structure) are related and both require that the structure of ASIC1b is significantly different form ASIC1a in the proximal part of the extracellular loop.

N192 and N216 of ASIC1b are predicted to localize to a short α-helix (α-helix 3) and at the beginning of a short β-sheet (β-sheet 4) of the finger and β-ball domains, respectively [5]. The side chains of the corresponding amino acids in chicken ASIC1 (D160 and D184) are both on the surface of the protein core in close proximity (~18 Å) to each other (Fig. 1B). D160 seems to be more readily accessible than D184, which is in a minor groove and partially shielded on one side by K205 (R235 in ASIC1b) and on the other side by the main chain (C180, S181, and P182 in chicken ASIC1 and C212, G213, and P214 in rat ASIC1b). Assuming that the protein structure in this part of the ectodomain is indeed different between ASIC1b and ASIC1a, the exact position of these amino acids may well be different in ASIC1b, however, and glycans may assist in adopting the proper conformation of the proximal ectodomain of ASIC1b. C180 of chicken ASIC1 forms a disulfide bridge with C173; in ASIC1b, glycans may, for example, influence formation of this bridge.

The two proximal glycosylation sites are at the very end of the region that is different between ASIC1a and ASIC1b [7, 8], immediately upstream of the splice-junction that connects the variable exon to the common exons of ASIC1a and 1b (Fig. 4A). This part of the ectodomain has been proposed to be the binding site of the spider toxin PcTx1 on ASIC1a [25] or, alternatively, to determine the functional consequences of PcTx1 binding to ASIC1a and 1b [26]. These proposals are in agreement with our interpretation that the differential glycosylation in the proximal ectodomain reflects structural differences in this region. The additional glycans on ASIC1b do not simply prevent binding of PcTx1, however, since PcTx1 also binds to ASIC1b [26].

Proximal glycosylation sites are present also in other ASICs. The second of the two proximal glycosylation sites of ASIC1b (N216) is conserved in ASIC2b, ASIC3, and ASIC4 (Fig. 1A). ASIC1b glycosylation may thus be prototypical for a subgroup of ASICs and proximal glycosylation sites may assist in folding or stabilize the structure of all members within this subgroup. ASIC4 is distinguished from other ASICs by the presence of 8 consensus sequences for *N*-glycosylation, scattered over its ectodomain (Fig. 1A). Treatment of ASIC4 with PNGase F reduces its molecular weight by more than 10 kD (I.K. & S.G., unpublished), suggesting that most of these sites indeed carry glycans. This result suggests that the structure of the ASIC4 ectodomain may be substantially different from that of other ASICs. Given that ASIC4 is not gated by H^+ and that its activation mechanism is still unknown [12–14], this is a likely hypothesis.

In summary, we propose that *N*-glycosylation makes an important contribution in shaping the structure of the proximal ectodomain of several ASICs.

Acknowledgements

This study was supported by DFG grant GR1771/3-4 to S.G.

REFERENCES

1 Waldmann, R. and Lazdunski, M. (1998) H(+)-gated cation channels: neuronal acid sensors in the NaC/DEG family of ion channels. Curr Opin Neurobiol **8**, 418-424

2 Wemmie, J. A., Price, M. P. and Welsh, M. J. (2006) Acid-sensing ion channels: advances, questions and therapeutic opportunities. Trends Neurosci **29**, 578-586

3 Lingueglia, E. (2007) Acid-sensing ion channels in sensory perception. J Biol Chem **282**, 17325-17329

4 Saugstad, J. A., Roberts, J. A., Dong, J., Zeitouni, S. and Evans, R. J. (2004) Analysis of the membrane topology of the acid-sensing ion channel 2a. J Biol Chem **279**, 55514-55519

5 Jasti, J., Furukawa, H., Gonzales, E. B. and Gouaux, E. (2007) Structure of acid-sensing ion channel 1 at 1.9 A resolution and low pH. Nature **449**, 316-323

6 Firsov, D., Robert-Nicoud, M., Gründer, S., Schild, L. and Rossier, B. C. (1999) Mutational analysis of cysteine-rich domains of the epithelium sodium channel (ENaC). Identification of cysteines essential for channel expression at the cell surface. J Biol Chem **274**, 2743-2749

7 Chen, C. C., England, S., Akopian, A. N. and Wood, J. N. (1998) A sensory neuron-specific, proton-gated ion channel. Proc Natl Acad Sci U S A **95**, 10240-10245

8 Bässler, E. L., Ngo-Anh, T. J., Geisler, H. S., Ruppersberg, J. P. and Gründer, S. (2001) Molecular and functional characterization of acid-sensing ion channel (ASIC) 1b. J Biol Chem **276**, 33782-33787

9 Waldmann, R., Champigny, G., Bassilana, F., Heurteaux, C. and Lazdunski, M. (1997) A proton-gated cation channel involved in acid-sensing. Nature **386**, 173-177

10 Yermolaieva, O., Leonard, A. S., Schnizler, M. K., Abboud, F. M. and Welsh, M. J. (2004) Extracellular acidosis increases neuronal cell calcium by activating acid-sensing ion channel 1a. Proc Natl Acad Sci U S A **101**, 6752-6757

11 Babini, E., Paukert, M., Geisler, H. S. and Gründer, S. (2002) Alternative splicing and interaction with di- and polyvalent cations control the dynamic range of acid-sensing ion channel 1 (ASIC1). J Biol Chem **277**, 41597-41603.

12 Gründer, S., Geissler, H. S., Bässler, E. L. and Ruppersberg, J. P. (2000) A new member of acid-sensing ion channels from pituitary gland. Neuroreport **11**, 1607-1611

13 Akopian, A. N., Chen, C. C., Ding, Y., Cesare, P. and Wood, J. N. (2000) A new member of the acid-sensing ion channel family. Neuroreport **11**, 2217-2222

14 Chen, X., Polleichtner, G., Kadurin, I. and Gründer, S. (2007) Zebrafish Acid-sensing Ion Channel (ASIC) 4, Characterization of Homo- and Heteromeric Channels, and Identification of Regions Important for Activation by H+. J Biol Chem **282**, 30406-30413

15 Helenius, A. and Aebi, M. (2004) Roles of N-linked glycans in the endoplasmic reticulum. Annu Rev Biochem **73**, 1019-1049

16 Hebert, D. N., Garman, S. C. and Molinari, M. (2005) The glycan code of the endoplasmic reticulum: asparagine-linked carbohydrates as protein maturation and quality-control tags. Trends Cell Biol **15**, 364-370

17 Kundra, R. and Kornfeld, S. (1999) Asparagine-linked oligosaccharides protect Lamp-1 and Lamp-2 from intracellular proteolysis. J Biol Chem **274**, 31039-31046

18 Turner, K. M., Wright, L. C., Sorrell, T. C. and Djordjevic, J. T. (2006) N-linked glycosylation sites affect secretion of cryptococcal phospholipase B1, irrespective of glycosylphosphatidylinositol anchoring. Biochim Biophys Acta **1760**, 1569-1579

19 Jansen, S., Callewaert, N., Dewerte, I., Andries, M., Ceulemans, H. and Bollen, M. (2007) An essential oligomannosidic glycan chain in the catalytic domain of autotaxin, a secreted lysophospholipase-D. J Biol Chem **282**, 11084-11091

20 Gründer, S., Firsov, D., Chang, S. S., Jaeger, N. F., Gautschi, I., Schild, L., Lifton, R. P. and Rossier, B. C. (1997) A mutation causing pseudohypoaldosteronism type 1 identifies a conserved glycine that is involved in the gating of the epithelial sodium channel. EMBO J **16**, 899-907

21 Paukert, M., Sidi, S., Russell, C., Siba, M., Wilson, S. W., Nicolson, T. and Gründer, S. (2004) A family of acid-sensing ion channels from the zebrafish: widespread expression in the central nervous system suggests a conserved role in neuronal communication. J Biol Chem **279**, 18783-18791.

22 Chen, X. and Gründer, S. (2007) Permeating protons contribute to tachyphylaxis of the acid-sensing ion channel (ASIC) 1a. J Physiol **579**, 657-670

23 Allen, S., Naim, H. Y. and Bulleid, N. J. (1995) Intracellular folding of tissue-type plasminogen activator. Effects of disulfide bond formation on N-linked glycosylation and secretion. J Biol Chem **270**, 4797-4804

24 Petrescu, A. J., Milac, A. L., Petrescu, S. M., Dwek, R. A. and Wormald, M. R. (2004) Statistical analysis of the protein environment of N-glycosylation sites: implications for occupancy, structure, and folding. Glycobiology **14**, 103-114

25 Salinas, M., Rash, L. D., Baron, A., Lambeau, G., Escoubas, P. and Lazdunski, M. (2006) The receptor site of the spider toxin PcTx1 on the proton-gated cation channel ASIC1a. J Physiol **570**, 339-354

26 Chen, X., Kalbacher, H. and Gründer, S. (2006) Interaction of acid-sensing ion channel (ASIC) 1 with the tarantula toxin psalmotoxin 1 is state dependent. J Gen Physiol **127**, 267-276

FIGURE LEGENDS

Figure 1 Positions of consensus sites for *N*-glycosylation of ASICs.
(A) Scheme showing the positions of putative consensus sites for *N*-glycosylation of different ASICs. Symbols with an identical color mark glycosylation sites at corresponding positions. **(B) Top,** scheme showing the positions of the two distal consensus sites for *N*-glycosylation of chicken ASIC1. The positions of the two proximal sites of ASIC1b are shown as dashed lines; they are not glycosylated in chicken, however, because the consensus site is not conserved. The position corresponding to the insertion site of the HA epitope in ASIC1a and 1b is shown by an arrowhead. **Bottom,** ribbon diagram of the trimeric chicken ASIC1 structure (PDB entry 2QTS) [5] with subunits coloured magenta, cyan and yellow; only the ectodomains are shown. For one subunit, the N-acetylglucosamines of the two distal glycans together with the connecting asparagine residues are shown in all-bonds representation with carbon atoms in green, oxygen in red and nitrogen in blue and the positions corresponding to the two proximal glycans of ASIC1b are highlighted by green spheres. Similarly, the position where the HA epitope was introduced into the ectodomain of ASIC1a and 1b is marked by two red spheres.

Figure 2 Immunoblot analysis of *N*-linked glycosylation of ASIC1a
(A) Linear scheme of ASIC1a showing the approximate positions of *N*-glycans. M1 and M2, membrane spanning domains; HA, hemagglutinin epitope. **(B)** Effect of Endo H and PNGase F on apparent mass of ASIC1a. Samples of ASIC1a untreated with enzymes (lanes 1 and 4) were loaded in parallel with Endo H- or PNGase F-treated samples (lanes 2 and 3). **(C)** Immunoblot analysis of ASIC1a-wt (lane 1), -N366A (lane 2), -N393S (lane 3), and -

N366A/N393S (lane 4) mutants, showing that both *N*-glycosylation sites carry glycans. ASIC1a was detected with an anti-HA antibody. The results shown in panels (B) and (C) are representative for 3 independent experiments.

Figure 3 Mean current amplitudes and apparent H^+-affinity of ASIC1a glycosylation mutants.
(A) Representative current traces of ASIC1a and its glycosylation mutants. Scale bars correspond to 0.5 μA and 10 sec, respectively. **(B)** Bar graph showing peak current amplitudes (mean ± S.E.M.) at pH 5.0 for ASIC1a and its glycosylation mutants (n = 12 oocytes from 2 frogs; **, $p < 0.01$). **(C)** Concentration-response curves for ASIC1a wild-type (open circles), ASIC1a-N366A (gray squares), ASIC1a-N393S (gray circles) and ASIC1a-N366A/N393S (black squares). Solid lines represent fits to the Hill equation. All channels were untagged. n = 6 - 12 oocytes from 2 frogs.

Figure 4 Immunoblot analysis of *N*-linked glycosylation of ASIC1b.
(A) Linear scheme showing the approximate positions of *N*-glycans. The proximal part of the N-terminus, which differs from ASIC1a, is shown in dark grey. M1 and M2, membrane spanning domains; HA, hemagglutinin epitope; VSV, vesicular stomatitis virus epitope. **(B)** Effect of Endo H and PNGase F on apparent mass of ASIC1b. Samples of ASIC1b untreated with enzymes (lanes 1 and 4) were loaded in parallel with Endo H- and PNGase F- treated samples (lanes 2 and 3). **(C)** Immunoblot analysis of ASIC1b-wt (lanes 1 and 5), -N192A, -N216S, -N192A/N216S, -N399A, -N426S, and -N399A/N426S mutants (lanes 2 - 8). For "N1 - N4" all 4 glycosylation sites of ASIC1b were mutated (lane 9). ASIC1b was detected with an anti-HA antibody. The results shown in panels (B) and (C) are representative for 3 independent experiments.

Figure 5 Mean current amplitudes and apparent H^+-affinity of ASIC1b glycosylation mutants.
(A) Representative current traces of ASIC1b and its glycosylation mutants. Scale bars correspond to 1 μA (N216S: 0.1 μA) and 2 sec, respectively. **(B)** Bar graph showing peak current amplitudes (mean ± S.E.M.) at pH 4.5 for ASIC1b and its glycosylation mutants (n = 12 oocytes from 2 frogs; **, $p < 0.01$). Channels were tagged with the HA- and the VSV-epitope. **(C) Left**, concentration-response curves for ASIC1b wild-type (open circles), ASIC1b-N192A (gray squares), and ASIC1b-N216S (gray circles). n = 6 oocytes from 1 frog. **Right**, concentration-response curves for ASIC1b wild-type (open circles), ASIC1b-N399A (gray squares), ASIC1b-N426S (gray circles), and ASIC1b-N399A/N426S (black squares). n = 12 - 13 oocytes from 2 frogs. Solid lines represent fits to the Hill equation. Channels were tagged only with the VSV-epitope.

Figure 6 Surface expression of ASIC1b glycosylation mutants.
ASIC1b wild-type and ASIC1b glycosylation mutants were HA-tagged; untagged ASIC1b served as a control (first column). Results are expressed in RLUs/oocyte/sec (mean ± S.E.M.). n = 20 - 30 oocytes from 3 different frogs; **, $p < 0.01$.

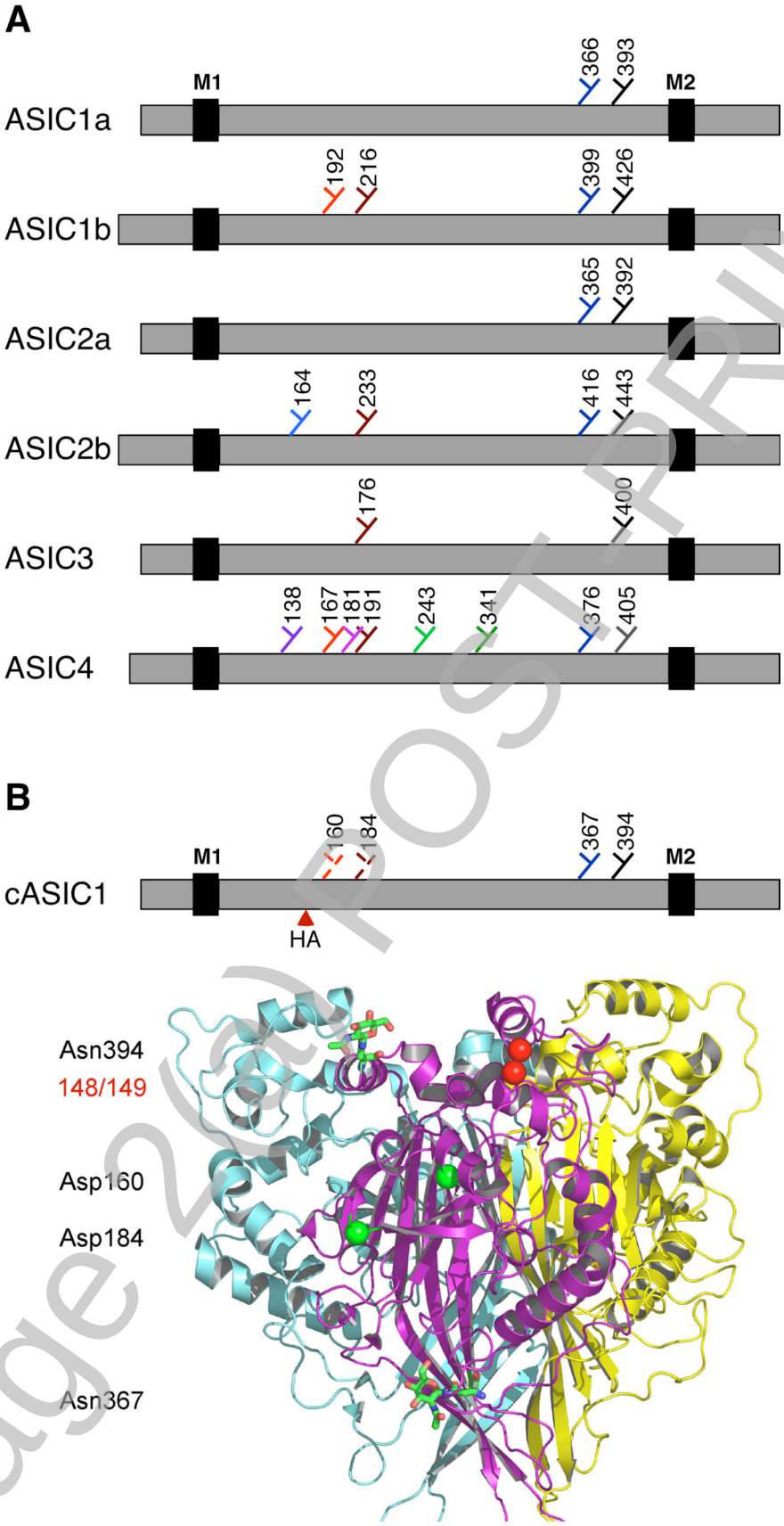

FIGURE 1

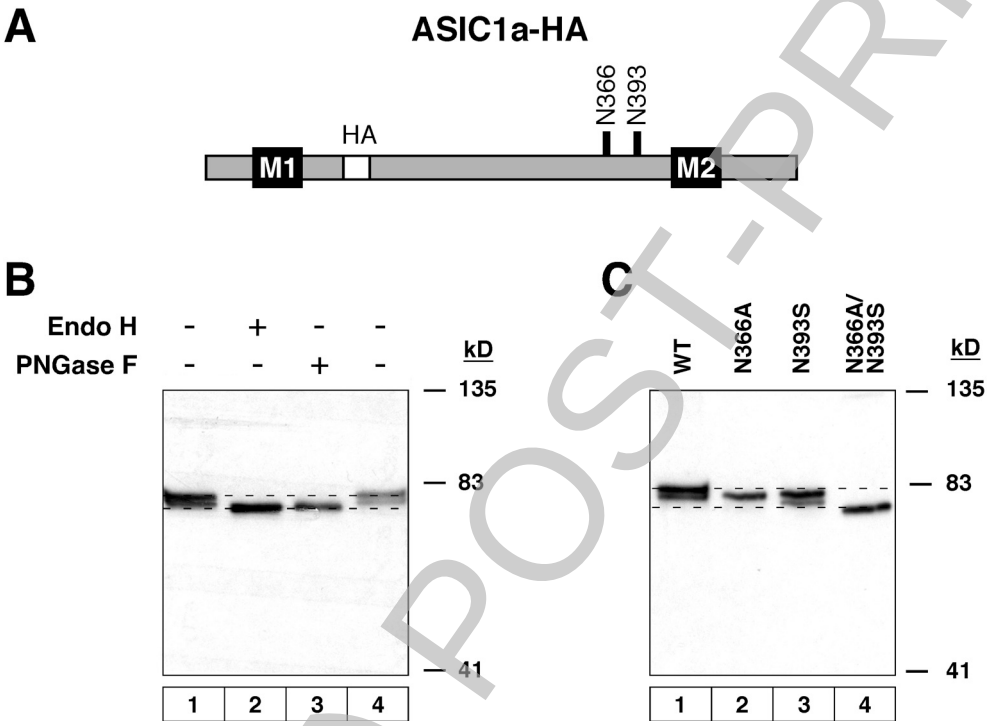

FIGURE 2

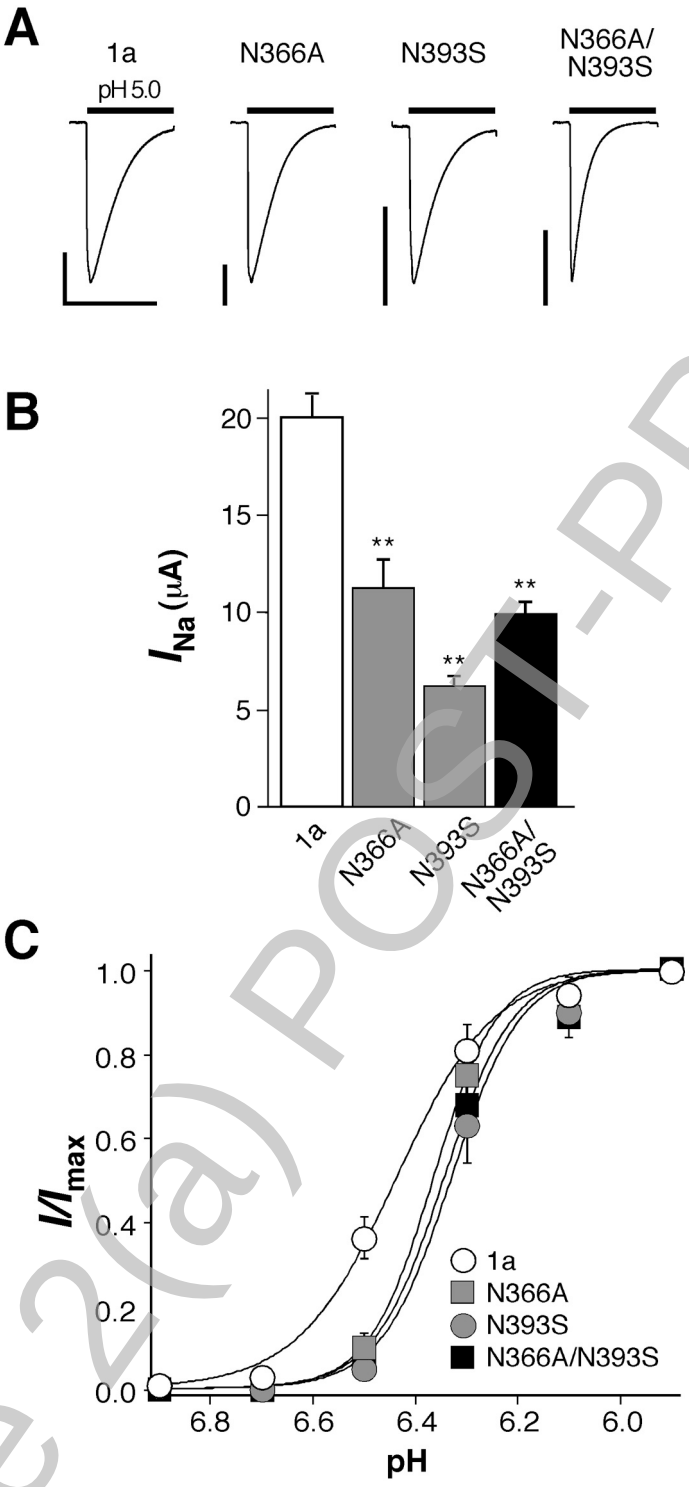

FIGURE 3

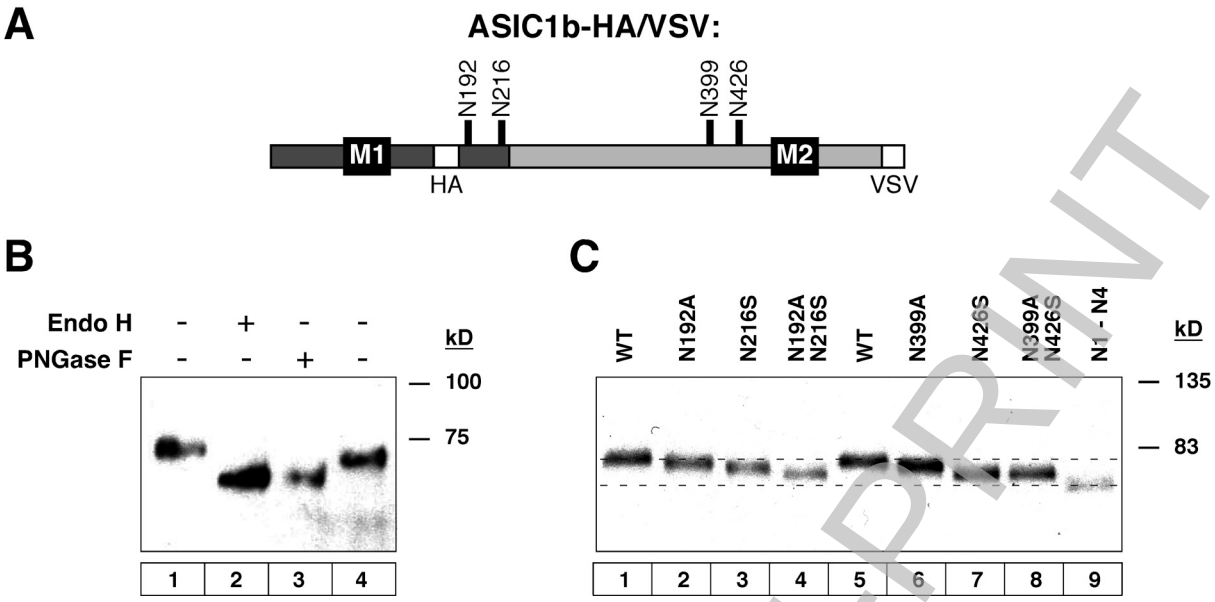

FIGURE 4

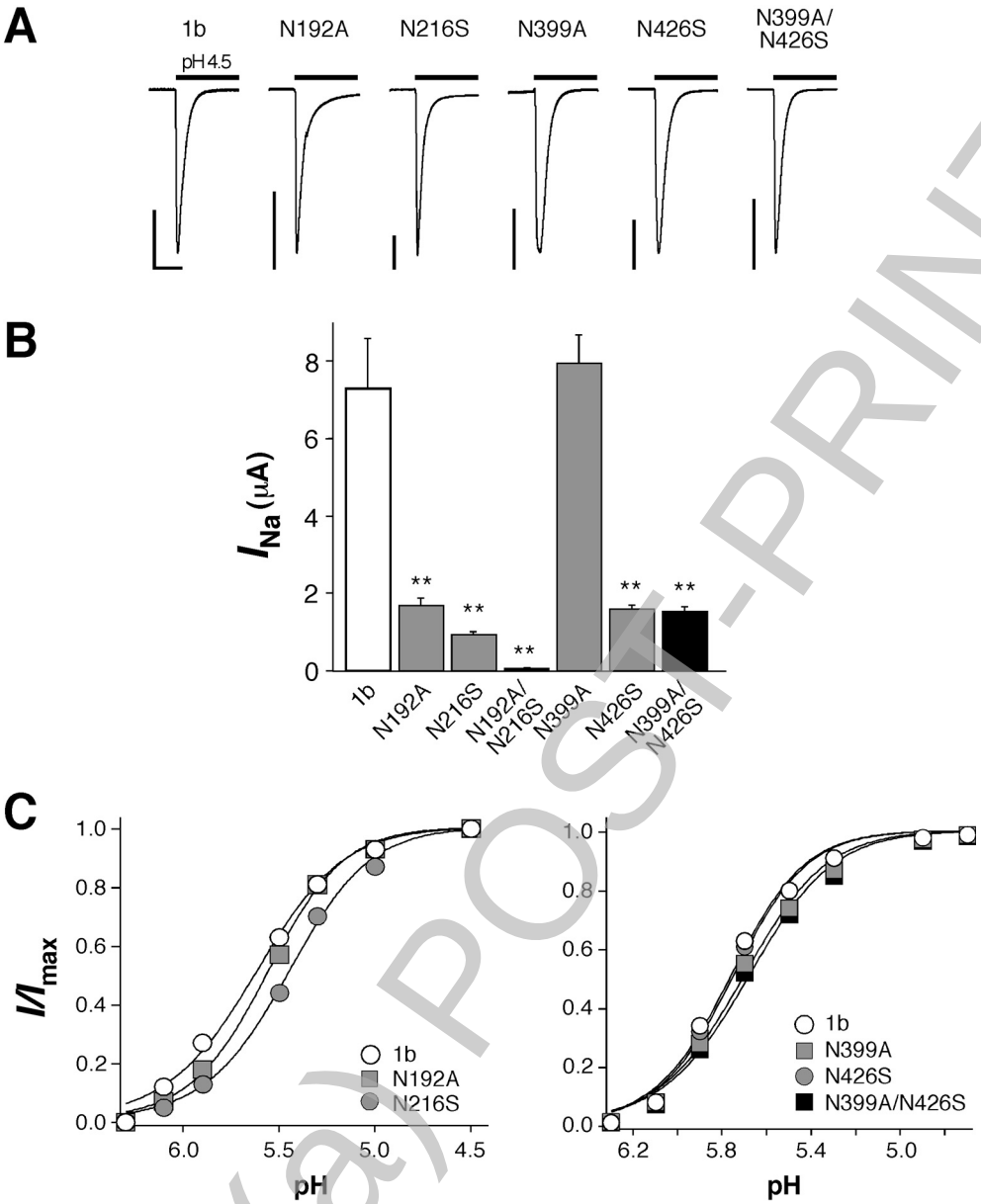

FIGURE 5

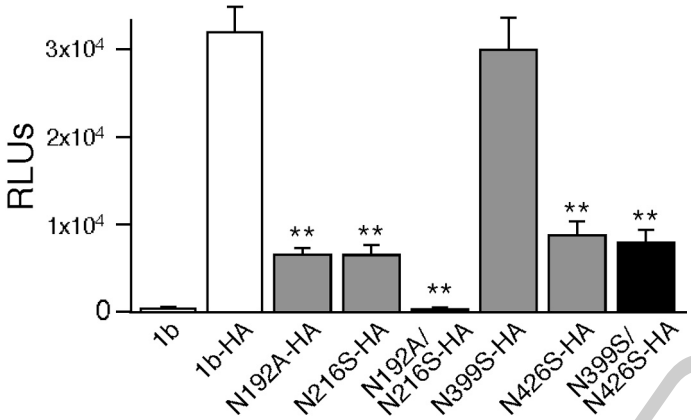

FIGURE 6